ELSEVIER

Catalysis Today 33 (1997) 335–352

CATALYSIS TODAY

FT-IR characterization of silicated aluminas, active olefin skeletal isomerization catalysts

Elisabetta Finocchio [a], Guido Busca [a], Stefano Rossini [b], Ugo Cornaro [b], Valerio Piccoli [b], Roberta Miglio [b]

[a] *Istituto di Chimica, Facoltà di Ingegneria, Università, Genova, P. le J.F. Kennedy, I-16129 Genoa, Italy*
[b] *Snamprogetti, via Maritano 26, I-20097 San Donato Milanese Milan, Italy*

Abstract

The surface structure of silicated aluminas, very good as catalysts for *n*-butene isomerization to isobutene, has been investigated by FT-IR spectroscopy of the silicate species, of the surface hydroxy-groups and of adsorbed pyridine. It has been concluded that silication results in the formation of a surface spinel phase where silicon substitutes for aluminum in tetrahedral sites. This phase exposes surface silanol groups that are not Brønsted acidic enough to protonate pyridine at room temperature. The increase in activity without loss in selectivity to isobutene is mainly attributed to the increased surface hydroxy-group concentration arising from silication, occurring without an increase in Brønsted acidity that would result in loss of selectivity and fast deactivation.

Keywords: FT-IR characterization; Silicated aluminas; Olefin skeletal isomerization catalysts

1. Introduction

Silicated alumina, patented in 1977 by Snamprogetti [1], has been the first generation catalyst, recently replaced by more performing systems [2], for the SISP-4 (skeletal isomerization Snamprogetti for C_4 olefins) commercial technology. The skeletal isomerization of *n*-butenes to isobutene can help to fulfil the increased demand of isobutene, whose availability has been foreseen as the bottle-neck of a growing request of ethers (MTBE, ETBE) for reformulated gasoline [3]. The chemical features of heterogeneously-catalyzed gas-phase *n*-butene skeletal isomerization have been studied by different authors particularly over pure and modified aluminas [4,5], but also over mixed oxides and zeolites [6–16], as recently reviewed by Butles and Nicolaides [17].

On the other hand, it has been found that silicated aluminas are by far more stable to sintering than pure aluminas [18,19] and this property, useful when reaction–regeneration cycles must be performed as in the case of butene skeletal isomerization, also suggested their use as catalyst supports for catalytic combustion technologies. Spectroscopic characterization studies of these materials appeared recently in the literature [4,5,19–22].

Upon an investigation aimed at the understanding of the basic chemical features of the *n*-butene skeletal isomerization process we un-

0920-5861/97/$32.00 Copyright © 1997 Elsevier Science B.V. All rights reserved.
PII S0920-5861(96)00106-X

dertook a study of the surface properties of silicated aluminas, very efficient catalysts for this reaction.

2. Experimental

Silicated alumina samples were prepared according to [1], using a commercial γ-Al_2O_3 powder (190 m^2/g, pore volume 0.48 ml/g, medium pore radius 85 Å, Na < 100 ppm; Si < 0.02%) as the support. The catalyst preparation, based on the chemical reaction of the activated support with tetraethylorthosilicate (TEOS) in ethanol solution, followed by distillation, hydrolysis and calcination at 823 K, has been optimized with respect to that described in the original patents. The samples considered in this paper contain up to 2.6% of SiO_2 (wt/wt) because in this range we found the most efficient catalysts. Hereinafter the samples will be denoted AX where X is the wt% of SiO_2. For comparison a 13% Al_2O_3-SiO_2 cracking catalyst from Strem has also been used.

The IR spectra were recorded with a Nicolet Magna 750 Fourier transform instrument (100 scans, 4 cm^{-1} resolution). The skeletal spectra in the region above 400 cm^{-1} have been recorded with KBr pressed disks and with a KBr beam splitter, while those in the far infrared region (400–50 cm^{-1}) have been recorded using the powder deposited on polyethylene disks, and with a 'solid substrate' beam splitter.

The adsorption experiments were performed using pressed disks of the pure powders, acti-

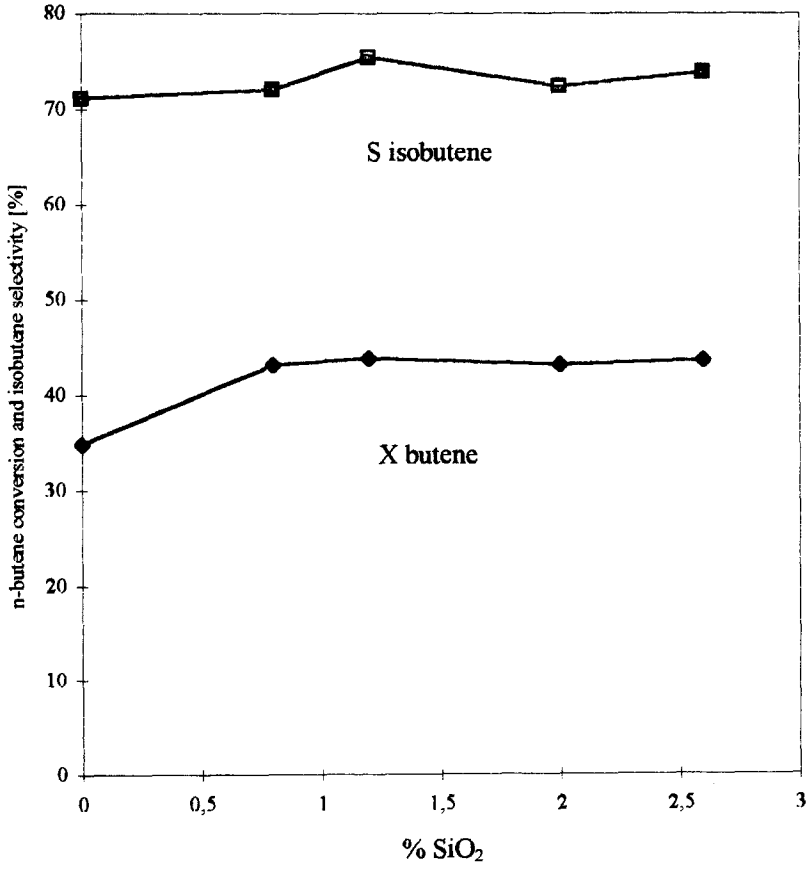

Fig. 1. *n*-Butene conversion (X) and isobutene selectivity (S) (%) over alumina and silicated aluminas.

vated by outgassing at 300–1070 K in the IR cell.

The catalytic tests reported here have been performed with pure butene 1 atm at 743 K taken from liquified 1-butene cylinders (LHSV 4.4 ± 0.1). The products have been integrally recovered from 20 min to 50 min time on stream and were analyzed by gas chromatography.

3. Results

3.1. Catalytic activity

In Fig. 1. the catalysts performances in *n*-butene isomerization at the conditions reported in the experimental section are reported. The *n*-butene conversion on pure alumina is 34.8% and increases to above 43% by silicon addition. Selectivity also slightly increases from 71% to above 75% for A1.2. The performances of the silicated aluminas raise nearly a plateau above 0.8% SiO_2. Conversion can be further increased by increasing total pressure and by decreasing space velocity, while selectivity is increased by decreasing total pressure and butene mole fraction in the feed, as well as by increasing space velocity. At optimum conditions, selectivities higher than 80% at about 37% conversion can be achieved over these silicated alumina catalysts. The data reported in Fig. 1 refer to the analysis of the integral reaction products from 20 to 30 min time on stream, which allows sufficient accuracy for analysis and reproducible and really significant reaction conditions. In the first 20 min, in fact, the initial activity is definitely higher but it steadily declines, due to partial catalyst deactivation. After 20 min catalytic activity decline, due to additional coke formation, is by far lowered. In the fixed bed industrial process the reactor is cyclically operated alternating reaction and regeneration conditions, with a complete restoring of the initial activity.

Under reaction conditions the equilibrium among 1-butene, *cis*-2-butene and *trans*-2-butene is immediately established. Side reactions give rise to C3 and C5 hydrocarbons, oligomers and C4 paraffins as the main byproducts, together with coke. A reaction network, based on the product analysis, is proposed in Scheme 1.

3.2. Skeletal catalyst spectra

The skeletal IR spectra of the alumina support and of the A2.6 silicated alumina measured

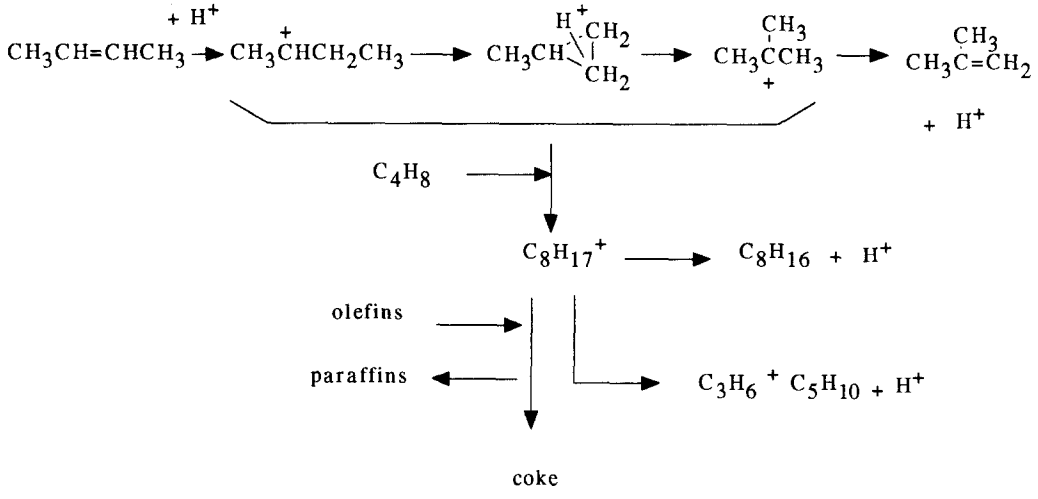

Scheme 1. Proposed reaction pathway for *n*-butene skeletal isomerization.

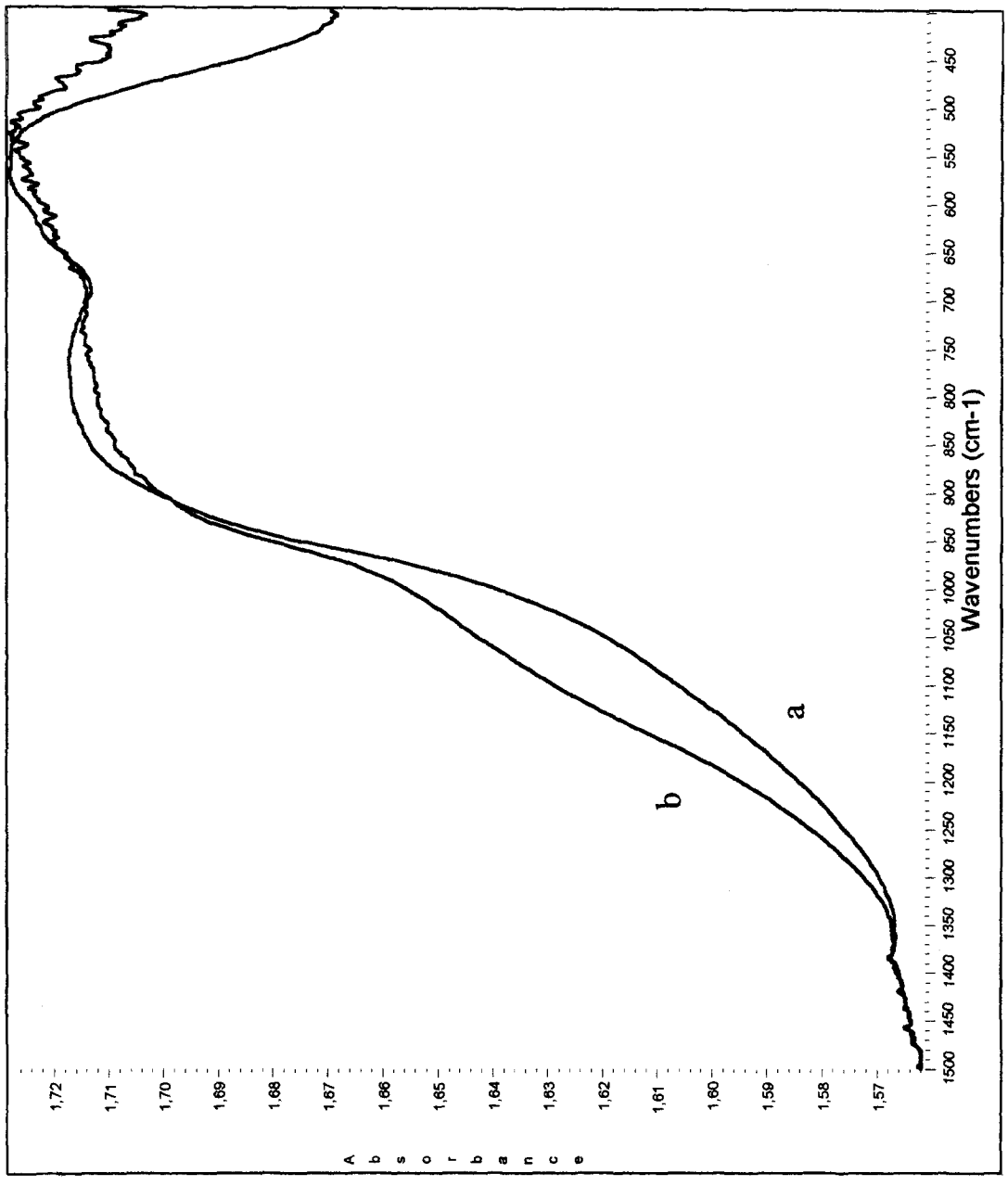

Fig. 2. FT-IR skeletal spectra of the pure support (a) and of the silicated A2.6 (b).

using KBr/polyethylene pressed disks are reported in Fig. 2. All spectra present the typical absorption of a transitional alumina in the region 1000–400 cm^{-1} [23–25]. The strength of the component near 850 cm^{-1} and the absence of sharp components supports the identification of this sample as being predominantly constituted by γ-Al_2O_3, in agreement with XRD data.

The silicated samples show an additional broad absorption evident as a more or less pronounced shoulder in the region 1300–800 cm^{-1}. The subtraction spectra, i.e. the spectra of the silicated samples from which the spectrum of the pure alumina support has been subtracted, are also compared in Fig. 3 with those of amorphous silica and silica-alumina. The subtraction spectra show a broad band with perhaps two components near 1040 and 1120 cm^{-1}, while a negative band appears near 950 cm^{-1}. Interestingly, no positive bands are found in the region 850–700 cm^{-1}.

The band in the region 1150–1000 cm^{-1} is clearly associated to Si–O stretching, present in this region in all silicate species. On the other hand the absence of bands in the 800–700 cm^{-1} region (where typically symmetric stretching of Si–O–Si bridges fall) strongly supports the idea that these species are not polymeric, only orthosilicate species being present [26]. In agreement with this interpretation, it is evident that the spectrum we observe definitely differs from those of amorphous silica and silica-alumina, also reported in Fig. 3, whose main maxima are sharp in the range 1120–1080 cm^{-1} with a pronounced shoulder near 1200 cm^{-1}, and where a band is also present near 800 cm^{-1}.

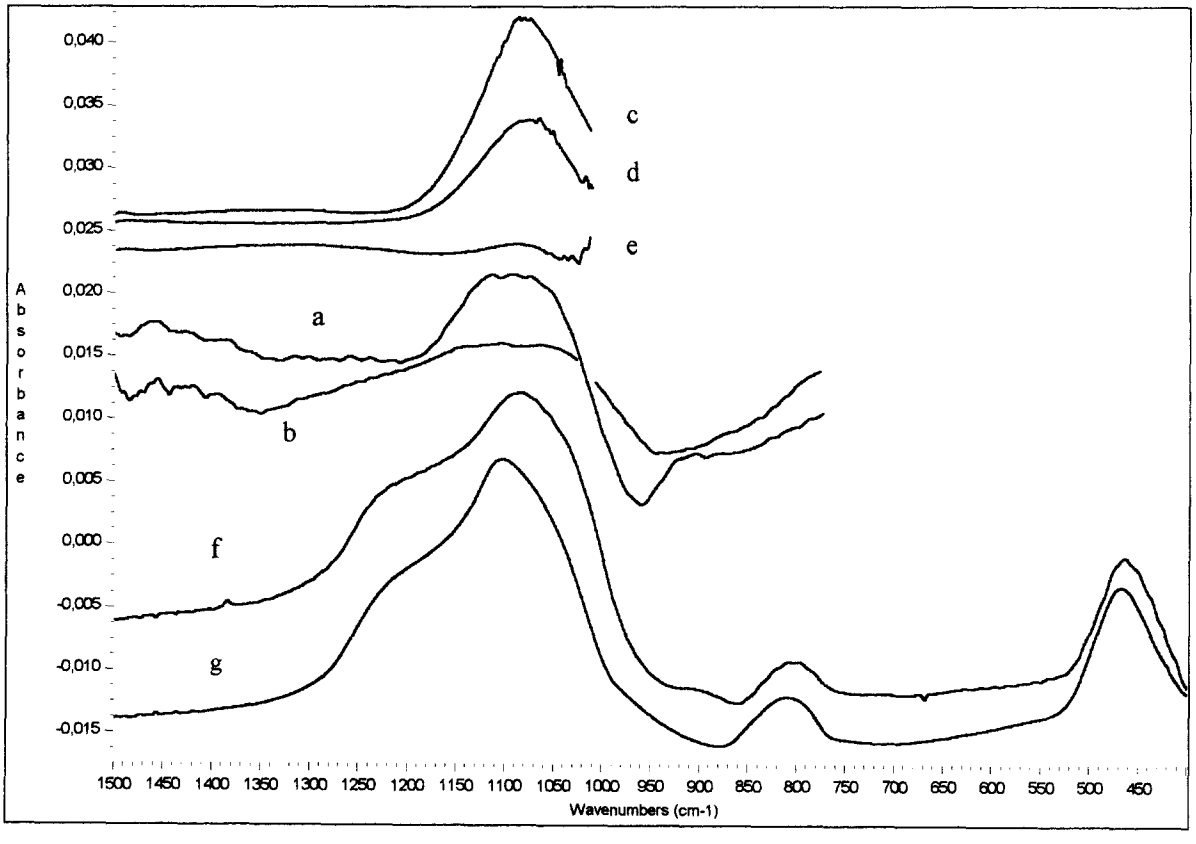

Fig. 3. Subtraction spectra A2.6-A (a, c), A0.8-A (d) and A0.4-A (b, e) for KBr pressed disks (a, b) and pure powders outgassed at 1000 K (c–e); (f) and (g) skeletal spectra of silica-alumina (13% Al_2O_3 from Strem) and of amorphous silica (Aerosil 200 from Degussa), respectively.

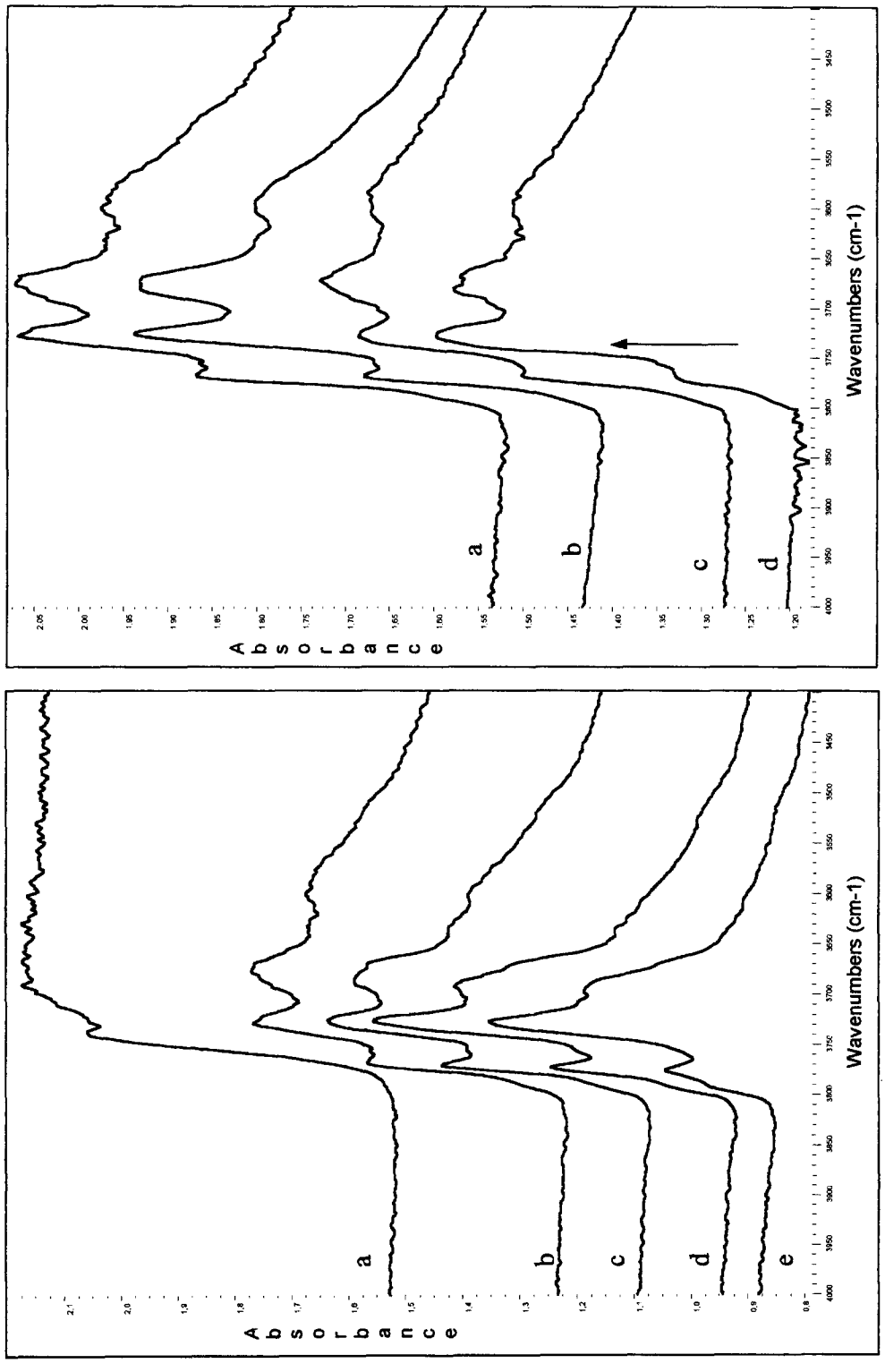

Fig. 4. (Left) FT-IR spectra (OH stretching region) of the pure alumina support after outgassing at 300 K (a), 720 K (b), 823 K (c), 923 K (d) and 1000 K (e). (Right) FT-IR spectra (OH stretching region) of the pure alumina (a) and of A0.4 (b), A 0.8 (c) and A2.6 (d) after outgassing at 720 K. The arrow shows an additional component in the spectra of silicated aluminas.

The negative band at 950 cm^{-1} in the subtraction spectra indicates that the absorption in this region is decreased by the addition of silica to alumina. The absorption in this region is typically due to the stretching of AlO_4 tetrahedra, as demonstrated by Tarte [23]. These features suggest that a surface phase is formed upon silication, with a lower occupancy of tetrahedral sites by Al atoms with respect to γ-Al_2O_3.

As usual, the pressed disks of pure aluminas (without binding materials like KBr) show a cut-off limit at 1000 cm^{-1}, due to the skeletal vibrations. However, above this cut-off the bands associated to adsorbed or surface species can be detected. In Fig. 3 the spectra of pressed disks of pure A2.6, A0.8 and A0.4 after subtraction of the spectrum of pure alumina are reported, after outgassing at 1000 K. The spectra of A2.6 and A0.8 clearly show a pronounced band near 1065 cm^{-1}, that is the same already observed for samples in KBr disks. The sample A0.4 also show this absorption, but with more difficulty, and evidences clearly a negative band near 1030 cm^{-1}. As shown by Morterra [27], Lavalley et al. [28] and Zecchina et al. [29], alumina disks contain in this region an absorption due to the asymmetric stretching of surface Al–O–Al bridges. More recent data allowed some of us to suggest that this absorption is due to Al–O modes involving tetrahedral Al cations, whose surface value is in the 1060–1000 cm^{-1}, range versus the unperturbed bulk value of near 950 cm^{-1} [30]. This absorption disappears by adsorption of several molecules, due to the relaxation of these bridges with a consequent shift down of this stretching mode towards the 'bulk' value. The subtraction spectrum of our A0.4 sample can be interpreted as due to the superimposition of the negative band due to the relaxation or disappearance of surface Al–O–Al bonds (with respect to pure alumina) and the positive band due to the new Si–O–Al bridges.

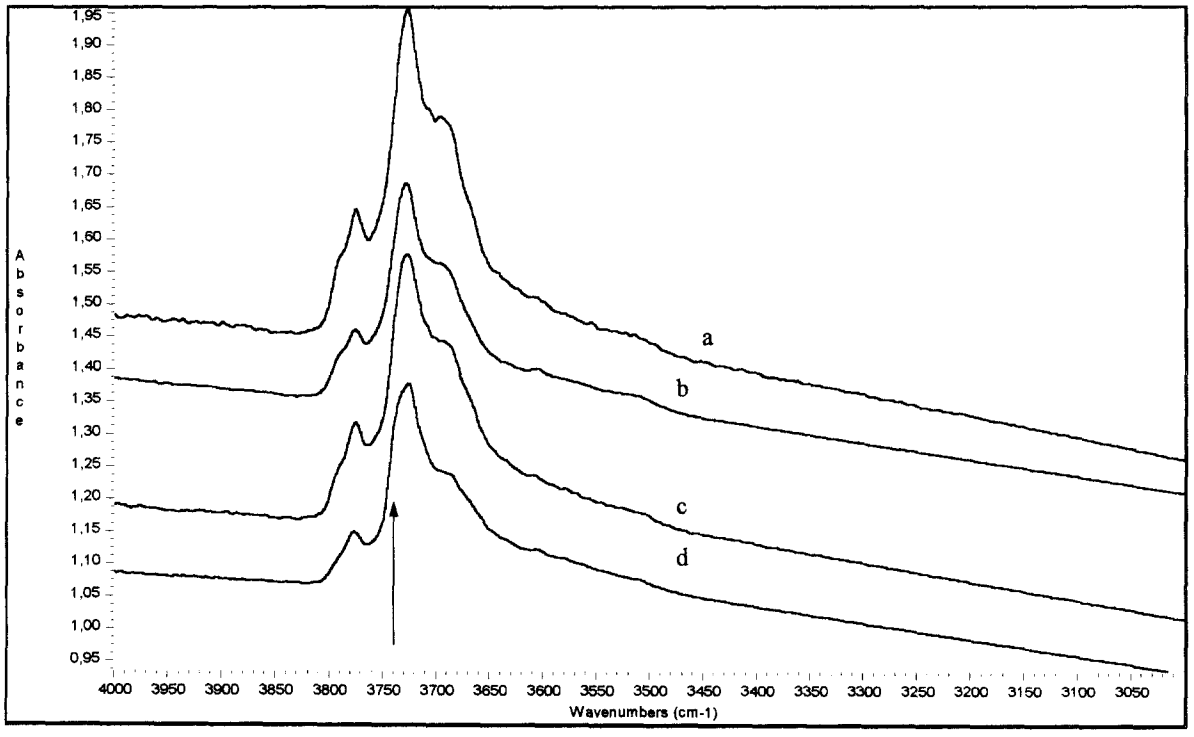

Fig. 5. FT-IR spectra (OH stretching region) of the pure alumina (a) and of A0.4 (b), A 0.8 (c) and A2.6 (d) after outgassing at 1000 K. The arrow shows an additional component in the spectra of silicated aluminas.

3.3. Surface hydroxy-groups

The FT-IR spectra of the pure alumina support in the OH stretching region, after different outgassing treatments are reported in Fig. 4(left).

As always for spinel-type transitional aluminas [31], if well outgassed, the spectrum of our sample outgassed at 1000 K shows at least four bands, near 3790 (shoulder), 3770, 3730 and 3680 cm^{-1}. A fifth broader band near 3590 cm^{-1} can be also seen after milder pretreatments. According to the previous work of some of us [25,32], where the model of Knözinger and Ratnasami [31] was partly modified, the bands at 3790 and 3770 cm^{-1} are assigned to terminal OH groups over one tetrahedrally coordinated Al ion, either in a non-vacant environment or near a cation vacancy, respectively; the band at 3730 cm^{-1} is assigned to a terminal OH over an octahedrally coordinated Al ion, while the bands at 3680 and 3590 cm^{-1} (the last observed broad after activation at 773 K) are assigned to bridging and triply-bridging OH groups, respectively.

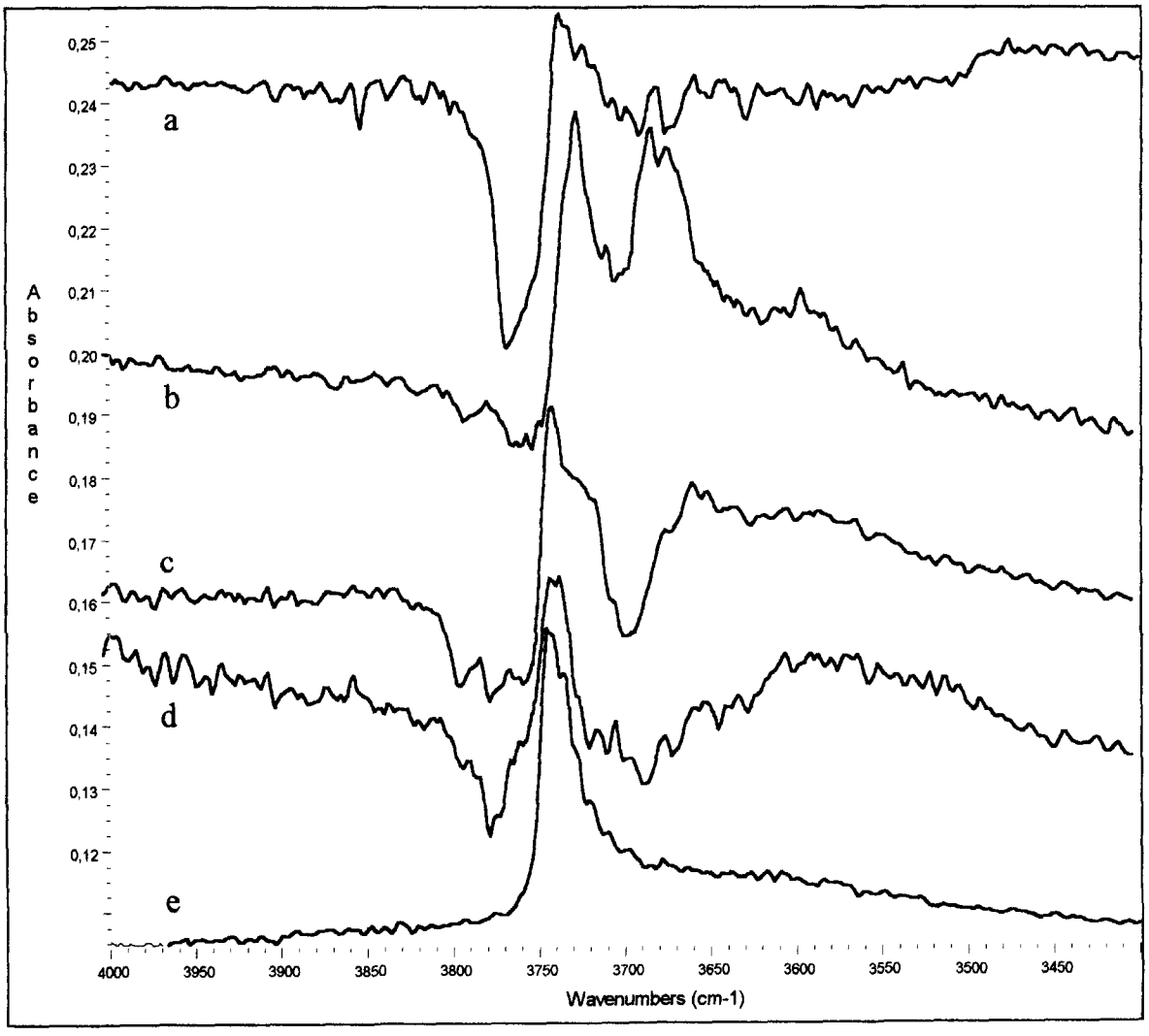

Fig. 6. Subtraction FT-IR spectra (OH stretching region): A2.6 support (outgassing at 720 K) (a); A0.4 support (outgassing at 720 K) (b); A2.6 support (outgassing at 1000 K) (c); A0.4 support (outgassing at 1000 K) (d); (e) FT-IR spectrum of an amorphous silica-alumina (13% Al_2O_3) from Strem, outgassed at 1000 K.

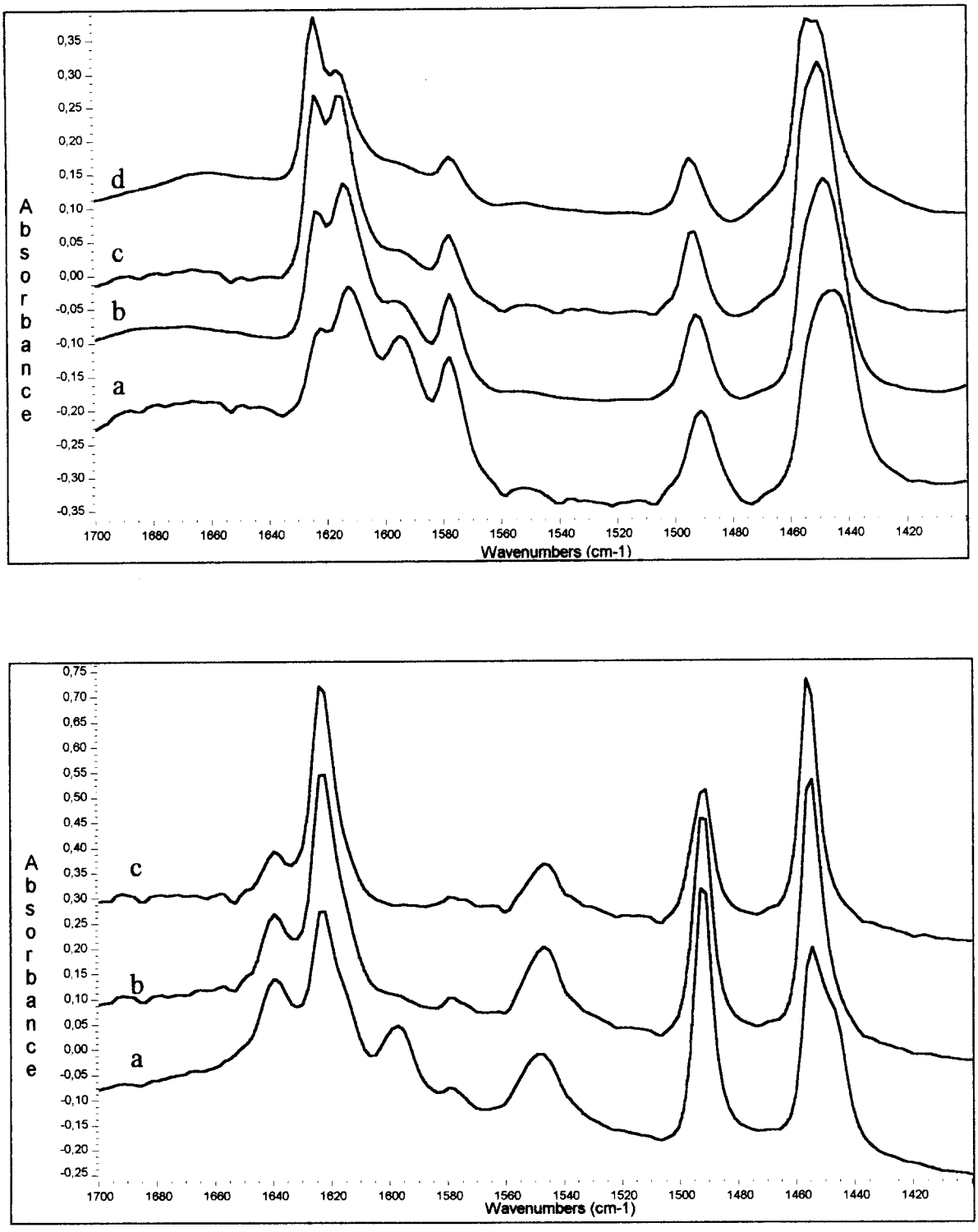

Fig. 7. (Top) FT-IR spectra of pyridine adsorbed over the pure alumina support; successive outgassing at 300 K (a); 373 K (b); 473 K (c); and 573 K (d), 30 min and (bottom) FT-IR spectra of pyridine adsorbed over the 13% silica-alumina; successive outgassing at 300 K (a); 373 K (b) and 473 K (c), 30 min.

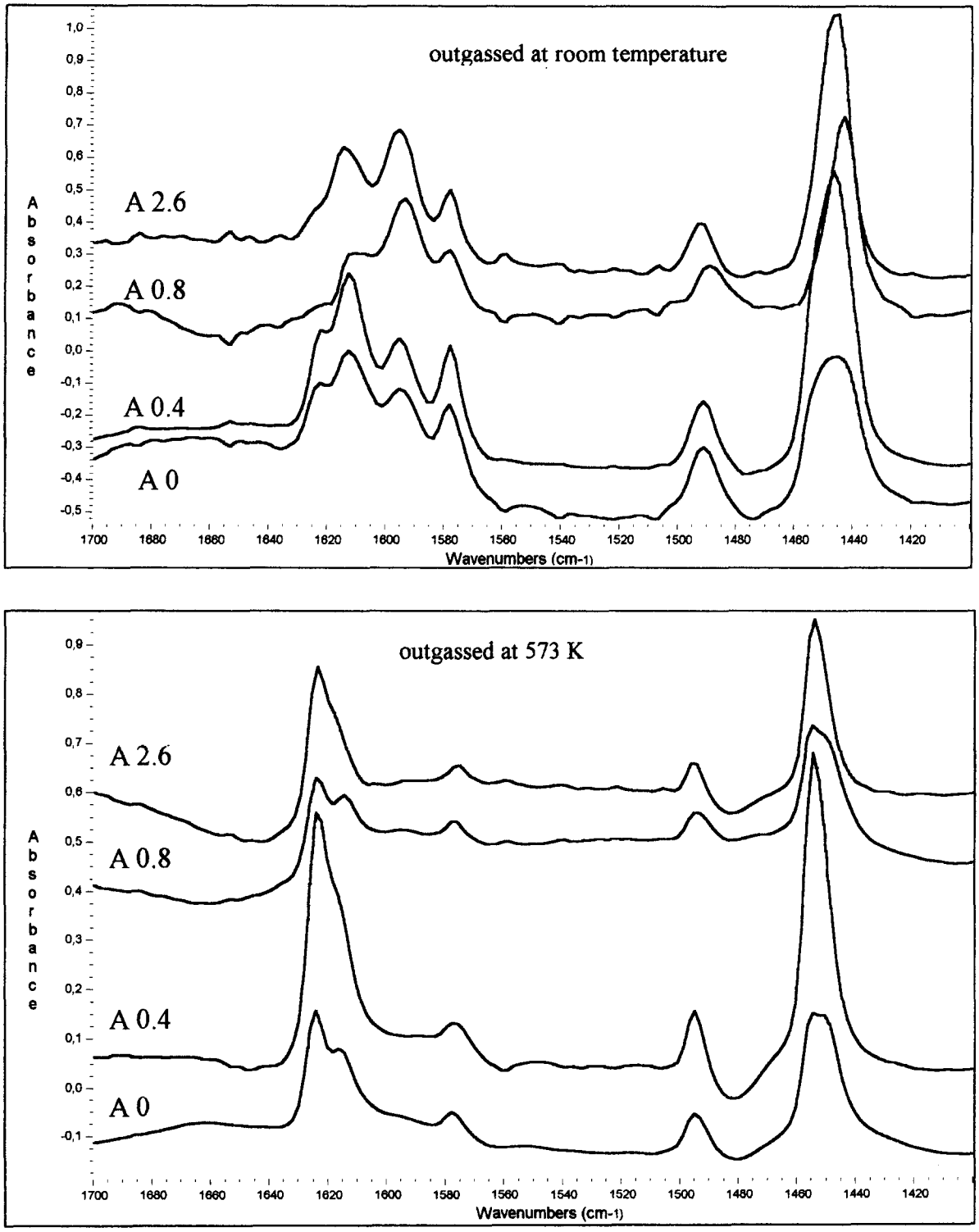

Fig. 8. FT-IR spectra of pyridine adsorbed over the pure alumina A0 and of A0.4, A 0.8 and A2.6 after outgassing at 300 K (upper spectra) and 573 K (lower spectra).

In Figs. 4 and 5 the spectra of the A0, A0.4, A0.8 and A2.6 all after outgassing at 720 K [Fig. 4(right)] and 1000 K (Fig. 5) are comparatively shown. They actually appear all very similar. However, the subtraction spectra (where the spectrum of the alumina sample has been subtracted from those of the silicated samples, Fig. 6) definitely show that in all cases a significant perturbation occurs. In all Si-containing samples a new sharp component is present at 3725–3739 cm^{-1}, shifting towards higher wavenumbers by increasing the Si content, while the components at 3790 and 3770 cm^{-1} of pure alumina are definitely decreased in intensity, so being evident as a negative band in the subtraction spectra. The new component at 3725–3739 cm^{-1} (that in the non-subtracted spectra actually appears as a non-resolved shoulder) falls in the typical region of the O–H stretching of surface silanol groups over silica containing materials, although on pure silicas as well as on silica-aluminas this band is typically found near 3745 cm^{-1}. This is shown in Fig. 6e for a commercial silica alumina sample. So, this band can be taken as an evidence of the presence of surface silanol groups over our slightly silicated samples. As already observed in the case of silicated titanias [33], the smaller is the silicon coverage, the lower is the OH stretching frequency. This can be interpreted as an effect of the higher ionicity of SiO–Al bonds with respect to SiO–Si, that results in a lower bond order of the O–H bond. We can mention that the catalysts characterized by Niwa et al. [20] and by Sheng et al. [22] contain more silica than ours and, accordingly, show the νOH silanol band near 3745 cm^{-1}.

Apparently, the growth of the band of surface silanols occurs mainly at the expense of the bands at 3790, 3770 cm^{-1}, assigned to surface hydroxy groups bonded to tetrahedral aluminum ions. So, we confirm that Si addition results in the formation of a surface phase where tetrahedral Al ions are less concentrated than at the surface of alumina, as proposed above on the basis of the skeletal IR spectra.

3.4. Characterization of the surface acidity

In Fig. 7(top) the spectra of pyridine adsorbed on the alumina support are reported. As is usually done [34–37] the 8a ring vibrational mode (1578 cm^{-1} in the liquid), whose position shifts upwards upon interaction depending on the strength of the adsorbing Lewis site, is taken as a measure of the Lewis acid strength of the different sites, allowing their identification. The spectra of pyridine adsorbed on transitional aluminas are similar each other [25,32,34–37], showing three 8a bands near 1625, 1615 and 1595 cm^{-1}, due to three different adsorbed species (the last one rather labile). The bands at 1625 and at 1590 cm^{-1} (bands I and III) are due, according to Morterra et al. [35,36] and to the previous work of some of us [25,32], to pyridine coordinated over tetrahedral and octahedral aluminum ions, respectively, being always present in spinel-type aluminas and aluminates. Obviously, the tetrahedral and octahedral coordination sphere of aluminum cations are completed by pyridine, so being incomplete before pyridine adsorption. The 8a mode of H-bonded pyridine can additionally contribute to band III. The band near 1615 cm^{-1} (band II), instead, is present only in defective aluminate spinels, like transition aluminas, and its intensity depends from the extent of cation deficiency [38]. For this reason it is assigned to pyridine species coordinated on a tetrahedral Al^{3+} ion placed near a cation vacancy, so being its Lewis acidity lowered.

As is well known, no Brønsted acidity is detectable by pyridine adsorption over 'pure' transitional aluminas.

The spectra of pyridine adsorbed on pure alumina and on silicated aluminas after outgassing at room temperature and at 573 K (after pyridine adsorption) are compared in Fig. 8. The spectra are clearly closely similar and closely correspond, mainly as the position of the bands is concerned. In particular, we do not find any evidence of Brønsted acidity also on silicated aluminas. This contradicts what occurs on

silica-aluminas like the commercial sample from Strem used for recording the spectra reported in Fig. 7(bottom). In this case Brønsted acidity is clearly present, as evidenced by the bands at 1635 and 1545 cm^{-1}, and by the higher strength of the band near 1490 cm^{-1}, all typical features of pyridinium cations.

However, significant differences are found in the spectra of molecularly adsorbed pyridine species between pure and silicated samples, as band intensities are concerned. When the spectra recorded after outgassing at room temperature are taken into account, the more evident effect of silicon addition is the strong increase of the 8a component near 1595 cm^{-1}, that is, on the samples A0.8 and A2.6 the most intense one. Under these conditions this band is associated to weakly bonded pyridine, and contains, according to previous studies [32–37], the features due to both H-bonded pyridine and pyridine coordinated over octahedral Al cations (band III). After outgassing at higher temperatures, instead, this band is as intense on silicated as on pure alumina. This indicates that silication mainly increases the relative amount of physisorbed (H-bonded) pyridine. This datum is also supported looking at the intensity of the 19b band near 1450 cm^{-1} that is definitely increased by silication when the spectra are recorded at room temperature but is not after outgassing at 573 K. This band is due to 'molecular' pyridine, i.e. to both Lewis bonded and H-bonded pyridine after outgassing at 300 K, while only to Lewis bonded pyridine after outgassing at 573 K.

In Fig. 9 the subtracted spectra upon pyridine adsorption on pure alumina and on A2.6 are shown in the overall IR spectral region. These spectra are those recorded upon pyridine adsorption, after subtraction of the spectra of the cor-

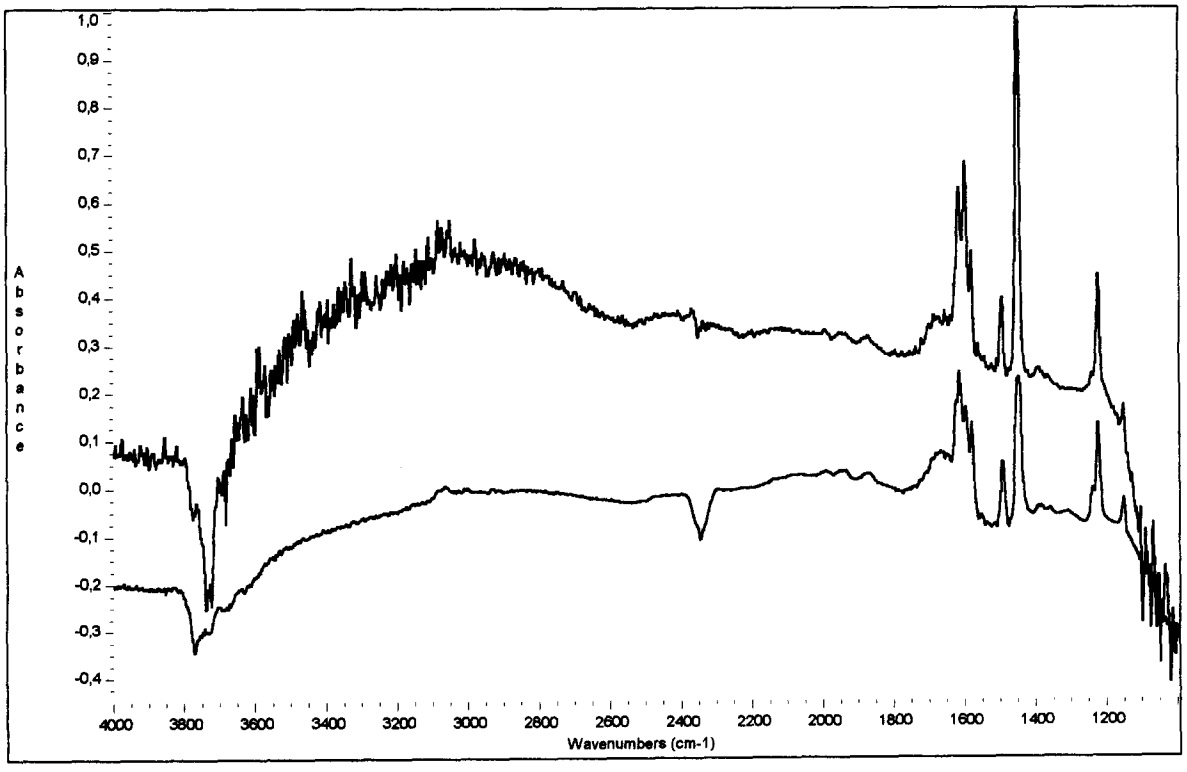

Fig. 9. Subtraction spectra relative to the adsorption of pyridine followed by outgassing at room temperature for pure alumina (lower spectrum) and A2.6 (upper spectrum). The spectra of the respective activated catalysts have been subtracted.

responding activated 'clean' catalysts. In the OH stretching region, sharp negative bands are observed that correspond to the bands of the free surface hydroxy groups that disappear upon pyridine adsorption (so, they become H-bonded). Over pure alumina, the negative band is that at 3770 cm^{-1}, with the shoulder near 3790 cm^{-1}. This can be interpreted as evidence that the hydroxy-groups primarily involved in H-bonding with pyridine are, on pure alumina, those bonded to tetrahedral Al cations. On A2.6 instead, the maximum of the negative band is at 3740 cm^{-1}, that means that the hydroxy-groups primarily involved in H-bonding with pyridine are, over silicated aluminas, the silanol groups. In the region 3600–1800 cm^{-1} a very broad 'positive' band dominates the spectrum. This absorption is apparently split into three components, with maxima near 3000, 2350 and 2100 cm^{-1} and minima near 2500 and 2200 cm^{-1}. This shape is typical of strong H bonds where the OH stretching band (νOH) becomes very broad and shifts downwards so strongly to interact with the first overtones of the in-plane and out-of-plane OH deformation modes (δOH and γOH, respectively) through a Fermi resonance [39,40]. The unperturbed position of these overtones is near the minima. This means that the position of the δOH and γOH fundamentals is, for the H-bonded OH groups in our case, near 1175 and 1050 cm^{-1}, respectively, which confirms the strength of this H-bonding interaction. In any case, the shape and the position of all these components over pure alumina and silicated aluminas are virtually identical. Nevertheless, the intensity of this absorption relative to the bands of Lewis-bonded pyridine (the bands at 1624 and 1615 cm^{-1}) is significantly stronger for silicated than for pure alumina.

These data agree with the previous ones by Basini et al. [5] that, by using a stronger basic probe like ammonia, only found small amounts of Brønsted sites, and with those of Niwa et al. [20] that concluded that the silanol groups over silicated aluminas are weak Brønsted sites, also at much higher coverages than ours. The spectra of pyridine adsorbed on silicated aluminas published by Nilsen et al. [4] do not differ very much from ours, only showing small traces of Brønsted-bonded pyridine, although these authors concluded that 'strongly acidic groups can be incorporated into the surface of Al_2O_3 as a result of condensation reactions with $[Si(OC_2H_5)_4]$'.

These data definitely support the impression that our silicated alumina samples do not present strong Brønsted sites similar to those found on amorphous silica-aluminas and protonic zeolites (in fact pyridine is not protonated) but contain a definitely higher number of surface hydroxy-groups than pure alumina (essentially the silanols) that are available for H-bonding with pyridine at room temperature.

Another detail which differentiates pure from silicated aluminas with respect to pyridine adsorption is that the 8a bands I and II (due to pyridine Lewis-bonded to two different tetrahedral Al sites) appear slightly less resolved, perhaps showing a higher disorder near tetrahedral cationic sites, in agreement with the silicon for aluminum substitution proposed to occur at these sites.

4. Discussion

4.1. On the structure of surface silicate species on silicated aluminas

The results discussed above allow us to hypothesize a structure for the supported silicate species on silicated aluminas. It seems evident that the preparation method gives rise to a specific reaction of TEOS on some surface hydroxy-groups (those bonded to tetrahedral Al, characterized by νOH at 3790 and 3770 cm^{-1}), and the formation of specific silicate species. These species are substantially homogeneous in the samples A0.4 to A2.6 and they are of the orthosilicate type, i.e. without Si–O–Si bridges. The area available for each Si atom (supposing they homogeneously distribute on the surface) is

near 75 Å^2 for the sample with the highest silica loading, 2.6% SiO_2, A2.6. This area can be compared with the area per Si atom in silicate structures. In the sheets of layer silicates like kaolinite the area per Si atom is no more than 11 Å^2 [41]. Previously, Imamura et al. [42] evaluated the area of a silicate unit as 25.4 Å^2, by comparison with that occupied in the cristobalite structure. A rough evaluation of the area occupied by an orthosilicate unit (with no oxygens bridging with other silicate units and Si–O distance 1.61 Å) allowed us to obtain 23 Å^2 for hydrogen-silicate species bonded with three oxygens to the alumina surface (species I, see below), and 20 Å^2 for dihydrogen silicate species bonded to the surface through two oxygens only (species II). According to these calculations, Si content in our A2.6 samples is sufficient to cover 1/3 of the alumina surface, at most. On the other hand, experimental data allowed Niwa et al. [29] to conclude that the full coverage of alumina by silica is obtained with 13 Si/nm^2, i.e. 7,7 Å^2 per Si atom. According to these data, the coverage in our samples is no more than 10% for A2.6.

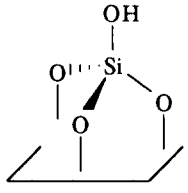

(I)

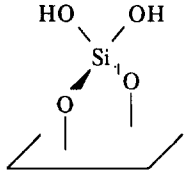

(II)

Models I and II represent reasonable structures of orthosilicate-type species supported on an oxide surface. These species can be formed by a reaction of TEOS with the surface hydroxy-groups of alumina:

$$n(\mathrm{Al-OH}) + \mathrm{Si(OEt)_4} \rightarrow (\mathrm{Al-O})_n\mathrm{Si(OEt)_{4-n}} + n\mathrm{EtOH}$$

The most probable value of n is 2, because its seems rather unlikely to find 3 hydroxy groups at the correct distance to give the reaction. The ethoxy-groups convert to hydroxy groups upon the successive hydrolysis and calcination, so that, from this point of view, species II could be taken as the more likely one.

However, it should also be remarked that upon calcination at 823 K, like in our experimental preparation, ion diffusion at the alumina surface is already possible, so that the surface can reconstruct and give rise to new structures. Structure I can be assumed to be more stable than structure II, so that structure II could easily transform into structure I if nearest oxide or hydroxide anions move slightly.

On the other hand, SiO_2 solubility in spinel-like alumina should be also taken into account. Indeed SiO_2 is slightly soluble in spinel-like alumina giving rise to a 'bulk' spinel type phase with composition near $SiO_2 \cdot 6Al_2O_3$ (equivalent to $Si_{0.2}Al_{2.4}O_4$) stable in the temperature range between 973 to 1373 K, recently characterized by Okada and Otsuka [43], whose IR spectra look similar to ours. Thus, according to the relatively high calcination temperature used in our catalyst preparation, it is possible to suppose that silica can penetrate from the surface towards the bulk of alumina, producing a layer of this spinel-like silica-alumina phase. According to the composition of this phase and the silica nominal content in our catalysts, it is possible to calculate that a 4 Å thick uniform layer of the $Si_{0.2}Al_{2.4}O_4$ spinel could be formed in the case of the A2 sample. The surface of this $Si_{0.2}Al_{2.4}O_4$ spinel phase, supposed to be formed, should expose hydrogen silicate species like in model III, that can be located on the

(111) spinel-type face, and dihydrogen silicate species like IV, that can be located on (001) spinel type faces.

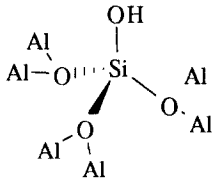

(III)

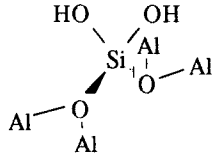

(IV)

Models III and IV, where the silicate species take part of the $Si_{0.2}$ $Al_{2.4}O_4$ surface layer, although similar to models I and II (where they stand up above the alumina surfaces), are perhaps more realistic. Moreover they agree perhaps better with the experimental observation that Si addition causes a slight decrease of the intensity of the absorption at 950 cm^{-1}, due to tetrahedral AlO_4 species, whose concentration should in fact decrease at the surface as an effect of silication.

Unfortunately, IR spectroscopy does not allow to distinguish geminal silanols (like those of II and IV), evidenced on SiO_2 surfaces by ^{29}Si CP/MAS NMR spectroscopy [44], from isolated terminal silanols (like those of I and III), as reported by Morrow [45]. From the evident asymmetry of the νOH band observed in our subtraction spectra (Fig. 7) we can suppose that in our case too we have both species, like on silica.

In any case, our data show that silica deposed on the alumina surface does not coalesce in the case of our catalysts in the form of silica or silica-alumina particles nor polymerize into polysilicate species. On the contrary, it strongly reacts with the alumina surface giving rise to orthosilicate species. This strong interaction is also responsible for hindering surface ion diffusion, with a stabilizing effect against sintering [18,19] useful, in the case of their use in olefin isomerization catalysis, to increase mechanical strength and stability with respect to reaction–regeneration cycles.

4.2. Surface chemistry and catalytic activity

The skeletal isomerization of n-butene and of higher olefins is well known to occur in liquid phase with sulphuric acid as the catalyst, and is thought to take place through transposition of the *sec*-butyl to the *tert*-butyl carbenium ion, likely involving a protonated methyl-cyclopropane carbonium ion as an intermediate [46]. The same mechanism likely occurs over solid acidic catalysts [15]. A reasonable reaction pathway based on our own experimental data is reported in Scheme 1.

As shown in Fig. 1, silication significantly increases *n*-butene conversion and also slightly increases selectivity to isobutene. As reported by Nilsen et al. [4], and confirmed in our laboratories, silicated aluminas are much more efficient than silica-aluminas in the skeletal isomerization of 1-butene, in spite of the stronger Brønsted acidity of the latter. On the other hand, it is well-known that silica-aluminas are efficient cracking catalysts for olefins [47], and these are reactions demanding stronger Brønsted acidity than skeletal isomerization. It seems consequently very likely that efficient catalysts for butene skeletal isomerization do not need to be very strong Brønsted acids just because in that case they also catalyze successive or parallel reactions (like oligomerization, cracking and coking) that limit selectivity and increase deactivation rate by coking.

According to these considerations, the above characterization experiments show that silicated aluminas are not stronger Brønsted acid solids than aluminas, within the sensitivity of our ex-

perimental method. However, silication appears to increase the number of active hydroxy groups stable on the surface after a given pretreatment. This allows to increase catalyst activity without decreasing selectivity.

In fact, surface hydroxy-groups are not indefinitely stable at the surface of an oxide but the higher is the temperature, the more they tend to desorb as water. Their concentration depends on i) the nature of the catalyst; ii) the water vapour pressure in contact with the catalyst; iii) the temperature. On pure γ-alumina the surface is still largely hydroxylated at 750 K (i.e. the reaction temperature), according to previous studies [48], although the hydroxyl-group concentration slowly decreases with time. This means that an equilibrium of the following reaction:

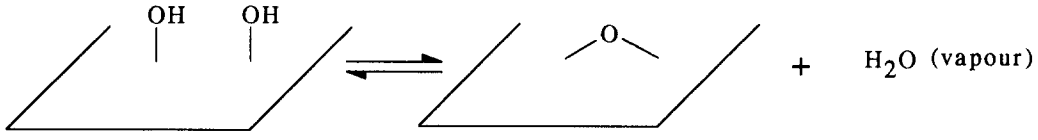

can be slowly established. However, it is obvious that, if the catalyst is modified so that the OH groups are more strongly bonded to the surface, this equilibrium can be shifted towards left. Literature data show that silica behaves very differently than alumina to dehydration. In fact, silica dehydrates almost completely at much higher temperatures than aluminas and only after these extremely hard treatments (outgassing above 1473 K) coordinatively unsaturated Si atoms acting as Lewis acid sites appear [49]. On the contrary, aluminas dehydrate substantially already at 1073 K and coordinatively unsaturated Al cations acting as very strong Lewis sites are observed after outgassing at very low temperature. This should indicate that Si–OH bonds are less easily broken than Al–OH bonds. Consequently, silication of alumina can give rise to surface silanols with higher stability with respect to the Al–OH groups of pure alumina, eventually allowing a higher concentration of active OH groups upon reaction conditions. The above equilibrium also explains the positive effect of some amounts of water vapour co-fed with the hydrocarbon stream, on catalytic activity of aluminas [15].

Concluding, it is proposed that silication provides isolated Si–OH bonds that are not significantly more acidic but more stable with respect to the desorption of water than Al–OH groups in reaction conditions. This results in the presence at the surface of a higher number of protons in any conditions, that, just because they are not strongly acidic, allow *n*-butene protonation and following transposition of the *sec*-butyl cation, faster than dimerization and cracking.

Thus, we conclude that alumina and silicated alumina act as Brønsted acid catalysts, although weak, in spite to the lack of detection of protonation of pyridine when it is adsorbed at room temperature. This is not a contradictory picture, because protonation of pyridine and protonation of olefins are related but very different phenomena. Protonation of pyridine is merely an acid–basic interaction, implying the involvement of a lone pair at nitrogen. On the other hand, stronger bases than pyridine (ammonia, piperidine) are protonated on alumina at room temperature. The hexothermic formation of a dative bond from the pyridine N lone pair with the proton arising from acidic OH groups is likely poorly affected by kinetics, and, consequently, occurs better at lower temperature than at higher temperature, according to thermodynamics. On the contrary, the formation of a carbenium ion from an olefin and a proton implies the breaking of the C = C π-type bond, the rehybridization of at least one carbon atom, and the formation of a new C–H σ-type bond. This much more complex process implies a activation energy and its rate is conse-

quently faster the higher the temperature is. Protonation of olefins over such catalysts is expected to occur at reaction temperature, i.e. 743 K. After carbenium ion formation, oligomerization, cracking and coking can occur.

5. Conclusions

The characterization of pure alumina and silicated aluminas highly selective in butene skeletal isomerization allows us to propose the following conclusions:

(i) Silication gives rise to isolated orthosilicate species strongly interacting with the spinel-type alumina structure, likely giving rise to a surface composition similar to that of the spinel $Si_{0.2}Al_{2.4}O_4$.

(ii) The formation of this phase gives rise to exposed silanol groups of hydrogen orthosilicate and/or dihydrogen orthosilicate species that are not more Brønsted acidic but more abundant than Al–OH groups and are available to hydrogen bonding with adsorbed bases.

(iii) The increased activity in butene conversion without a decrease in selectivity to isobutene observed by silication cannot be associated to a significant increase of Brønsted acidity (that would also increase the activity in the successive and/or competitive polymerization reactions so causing decrease of selectivity and, finally, catalyst coking and deactivation). It can essentially be associated to the increased amount of surface hydroxy groups stable in an adsorbed form also in reaction conditions (the silanols) that provide weakly acidic protons for the isomerization reaction occurring through carbenium ion formation.

(iv) Silicated aluminas are something very different from silica-aluminas and protonic zeolites, because the latter can be viewed as substitutional solid solutions of alumina (minor component) in tetrahedral silica frameworks while the former gives rise at the surface to a substitutional solid solution of silica in alumina (major component). Strong Brønsted acidity appears when Al^{3+} substitutes for tetravalent Si in the silica amorphous or crystalline framework, being associated to protons that compensate the corresponding charge defect. On the contrary, the charge excess occurring when tetravalent silicon substitutes for Al^{3+} in the tetrahedral sites of spinel-type aluminas is compensated by an increase of the defectivity of the spinel phase.

References

[1] F. Buonomo, V. Fattore and B. Notari, US Pat., 4013589 (1977); F. Buonomo, V. Fattore and B. Notari, US Pat., 4013590 (1977); G. Manara, V. Fattore and B. Notari, US Pat., 4038337 (1977).
[2] S. Rossini, D. Sanfilippo and R. Trotta, Proc. IXth Ital. Congr. Catalysis, Pisa, 1994, p. 208; Proc. Europacat II, Maastricht, 1995, p. 775.
[3] US Clean Air Act Amendments (Public Law 101-549, 15 November 1990).
[4] B.P. Nielsen, J.M. Onufrenko and B.C. Gates, Ind. Eng. Chem. Fundam., 27 (1986) 337.
[5] L. Basini, A. Aragno and A. Raffaelli, J. Phys. Chem., 95 (1991) 211.
[6] N.S. Raghavan and L.K. Doraiswamy, J. Catal., 48 (1977) 21.
[7] A.K. Ghosh and R.A. Kydd, Catal. Rev. Sci. Eng., 27 (1985) 539.
[8] Zheng X.C. and V. Ponec, J. Catal., 148 (1994) 607; Catal. Lett., 25 (1994) 337; 27 (1994) 113.
[9] P. Patrono, A. La Ginestra, G. Ramis and G. Busca, Appl. Catal. A General, 107 (1994) 249.
[10] L.H. Gielgens, M.G.H. vanKampen, M.M. Broek, R. van Hardeveld and V. Ponec, J. Catal., 154 (1995) 201.
[11] M.W. Simon, S.L. Suib and C.L. O'Young, J. Catal., 147 (1994) 484.
[12] H.H. Mooiweer, K.P. DeJong, B. Kraushaar-Czarnetzki, W.H.J. Stork and P. Grandvallet, Proc. Europacat-1, Montpellier, 1993, Paper A8.
[13] W.M. Ewert, E.L. Sughrue and M.D. Scharre, Proc. 1994 Annual AIChE Meeting, San Francisco, 1994, Paper 73b.
[14] J.B. Wise and D. Powers, in J.N. Armor, Editor, Environmental Catalysis, ACS, Washington D.C., 1994, p. 273.
[15] P. Grandvallet, K.P. DeJong, H.H. Mooiweer, A.G.T.G. Kortbeek and B.Kraushaar-Czarnetzki, EP Pat., 501577 (1992).
[16] H.H. Mooiweer, K.P. DeJong, B. Kraushaar-Czarnetzki and W.H.J. Stork, Stud. Surf. Sci. Catal., 84 (1994) 2327.
[17] A.C. Butler and C.P. Nicolaides, Catal. Today, 18 (1993) 443.
[18] M.F.L. Johnson, J. Catal., 123 (1990) 245.
[19] B. Beguin, E. Garbowski and M. Primet, J. Catal., 127 (1991) 595.
[20] M. Niwa, N. Katada and Y. Murakami, J. Phys. Chem., 94 (1990) 6441.

[21] T.C. Sheng and I.D. Gay, J. Catal., 145 (1994) 10.
[22] T.C. Sheng, S. Lang, B.A. Morrow and I.D. Gay, J. Catal., 148 (1994) 341.
[23] P. Tarte, Spectrochim. Acta, 23A (1967) 2127.
[24] G.A. Dorsey, Jr., Anal. Chem., 40 (1968) 971.
[25] G. Busca, V. Lorenzelli, G. Ramis and R.J. Willey, Langmuir, 9 (1993) 1492.
[26] H.H.W. Moenke, in V.C. Farmer, Editor, The Infrared Spectra of Minerals, The Mineralogical Society, London, 1974, p. 365.
[27] C. Morterra, Proc. 6th ICC, London, 1976, Royal Society of Chemistry, London, 1977.
[28] J.C. Lavalley and M. Benaissa, J. Chem. Soc., Chem. Commun., 908 (1984).
[29] A. Zecchina and D. Scarano, in M. Che and G.C. Bond, Editors, Adsorption and Catalysis on Oxide Surfaces, Elsevier, Amsterdam, 1985, p. 71.
[30] V. Sanchez Escribano, J.M. Gallardo Amores, E. Finocchio, M. Daturi and G. Busca, J. Mater. Chem., 5 (1995) 1943.
[31] H. Knözinger and P. Ratnasamy, Catal. Rev., 17 (1978) 31.
[32] G. Busca, V. Lorenzelli, V. Sanchez Escribano and R. Guidetti, J. Catal., 131 (1991) 167.
[33] Li Yi, G. Ramis, G. Busca and V. Lorenzelli, J. Mater. Chem., 4 (1994) 1755.
[34] H. Knözinger, H. Krietenbrink, H.D. Muller, and W. Schulz, Proc. 6th Int. Congr. Catalysis, Royal Society of Chemistry, London, 1976, p. 183.
[35] C. Morterra, S. Coluccia, A. Chiorino and F. Boccuzzi, J. Catal., 54 (1978) 348.
[36] C. Morterra, G. Ghiotti, F. Boccuzzi and S. Coluccia, J. Catal., 51 (1978) 299.
[37] C.Morterra, A.Chiorino, G.Ghiotti and E.Garrone, J. Chem. Soc., Faraday Trans. 1, 75 (1979) 271.
[38] G. Busca, V. Lorenzelli and V. Sanchez Escribano, Chem. Mater., 4 (1992) 595.
[39] S. Bratos and H. Ratajczak, J. Chem. Phys., 76 (1982) 77.
[40] C.U.I. Odenbrand, J.G.M. Brandin and G. Busca, J. Catal., 135 (1992) 505.
[41] D.T. Griffen, Silicate Crystal Chemistry, Oxford University Press, 1992.
[42] S. Imamura, S. Ishida, H. Tarumoto and Y. Saito, J. Chem. Soc., Faraday Trans., 89 (1993) 757.
[43] K. Okada and N. Otsuka, J. Am. Ceram. Soc., 69 (1986) 652.
[44] G.E. Maciel and D.W. Sindorf, J. Am. Chem. Soc., 102 (1980) 7607.
[45] B.A. Morrow, in J.L.G. Fierro, Editor, Spectroscopic Characterization of Heterogeneous Catalysts, Elsevier, 1990, Part a, p. 161.
[46] B.C. Gates, Catalytic Chemistry, Wiley, New York, 1992.
[47] B.W. Wojciechowski and A. Corma, Catalytic Cracking, Marcel Dekker, New York, 1986.
[48] J.B. Peri and R.B. Hannan, J. Phys. Chem., 64 (1960) 1526.
[49] B.A. Morrow and I.A. Cody, J. Phys. Chem., 80 (1976) 1995.